Supporting Information

AnB$_8^-$: Borozene Complexes with Monovalent Actinide

Wan-Lu Li*[a,b] and Jordan Burkhardt[a,c]

[a] Department of NanoEngineering University of California San Diego La Jolla, CA 92093 (USA)

[b] Program of Materials Science and Engineering, University of California San Diego, La Jolla, CA 92093 (USA)

[c] Department of Chemistry and Biochemistry, University of California San Diego La Jolla, CA 92093 (USA)

E-mail: wal019@ucsd.edu

Computational methods

Geometrical structures of both C_{7v} and C_s isomers were fully optimized using GGA-PBE[1] and hybrid PBE0[2] density functionals implemented in ADF 2023.102 package[3]. Vibrational frequencies were calculated to verify the true minimum on the potential energy surface. Slater-type basis sets with triple-ζ and one polarization term (TZP)[4] were applied treated by frozen-core approximation onto the inner shells [1s^2-5d^{10}] for actinides and [1s^2] for boron. To appropriately address the scalar relativistic effect, the zero-order regular approximation (ZORA)[5] was employed.

To account for the multiconfigurational character, we employed the complete active space self-consistent field method (CASSCF)[6] combined with a second-order perturbation treatment of dynamic electron correlation (N-electron valence perturbation theory to second order, NEVPT2)[7-11] using the ORCA 5.0.4 package[12, 13]. We utilized the SARC-TZVP[14] basis set for actinide elements and the def2-TZVP[15] basis set for the B element with the SARC/J[16] fitting basis set to expedite the calculation of integrals. Spin-orbit coupling effects were approximated by an effective one-particle operator[17, 18]. In AcB$_8^-$, the active space comprised one 7s orbital, 6d δ orbitals, 6d π orbitals, and their respective B group orbital counterparts, constituting a CAS (6e, 7o) active space. For other AnB$_8^-$ species, the active orbital space consisted of the An 5f, 7s, 6d π and 6d δ valence shell orbitals and the corresponding B orbital counterparts, 14 active orbitals in total.

Electronic structure and chemical bonding analyses were mainly focused on the C_{7v} isomer to determine the stability and oxidation state. To quantitively elucidate the bonding mechanism between An and B$_8$ moieties, energy decomposition analysis–natural orbitals for chemical valence (EDA–NOCV)[19, 20] was performed. Another framework, principle interacting orbital (PIO) approach[21], was also employed to identify the "dominant interacting orbitals" that are semi-localized and chemical-intuitively interpretable utilizing the Gaussian 09 calculation.[22] In terms of aromatic properties, we carried out adaptive natural density partitioning (AdNDP) analysis[23] to illustrate the multi-center bonding based on the canonical molecular orbitals. Nucleus-independent chemical shift (NICS)[24] index was calculated to quantitively characterize the aromaticity.

References

1.   J. P. Perdew, K. Burke and M. Ernzerhof, *Phys. Rev. Lett.*, 1996, **77**, 3865.
2.   C. Adamo and V. Barone, *J. Chem. Phys.*, 1999, **110**, 6158-6170.
3.   ADF, 2023.102, SCM, Theoretical Chemistry, Vrijie Universiteit, Amsterdam, The Netherlands, (http://www.scm.com).
4.   E. van Lenthe and E. J. Baerends, *J. Comput. Chem.*, 2003, **24**, 1142-1156.
5.   E. van Lenthe, E. J. Baerends and J. G. Snijders, *J. Chem. Phys.*, 1993, **99**, 4597-4610.
6.   P.-Å. Malmqvist and B. O. Roos, *Chem. Phys. Lett.*, 1989, **155**, 189-194.
7.   M. Atanasov, D. Aravena, E. Suturina, E. Bill, D. Maganas and F. Neese, *Coord. Chem. Rev.*, 2015, **289-290**, 177-214.
8.   C. Angeli, R. Cimiraglia, S. Evangelisti, T. Leininger and J.-P. Malrieu, *J. Chem. Phys.*, 2001, **114**, 10252-10264.
9.   C. Angeli, R. Cimiraglia and J.-P. Malrieu, *Chem. Phys. Lett.*, 2001, **350**, 297-305.
10.   C. Angeli, R. Cimiraglia and J.-P. Malrieu, *J. Chem. Phys.*, 2002, **117**, 9138-9153.
11.   C. Angeli, B. Bories, A. Cavallini and R. Cimiraglia, *J. Chem. Phys.*, 2006, **124**.
12.   F. Neese, *WIREs Computational Molecular Science*, 2012, **2**, 73-78.
13.   F. Neese, *WIREs Computational Molecular Science*, 2022, **12**, e1606.
14.   D. A. Pantazis and F. Neese, *J. Chem. Theory Comput.*, 2011, **7**, 677-684.
15.   F. Weigend and R. Ahlrichs, *Phys. Chem. Chem. Phys.*, 2005, **7**, 3297-3305.
16.   F. Weigend, *Phys. Chem. Chem. Phys.*, 2006, **8**, 1057-1065.
17.   B. A. Heß, C. M. Marian, U. Wahlgren and O. Gropen, *Chem. Phys. Lett.*, 1996, **251**, 365-371.
18.   F. Neese, *J. Chem. Phys.*, 2005, **122**.
19.   M. P. Mitoraj, A. Michalak and T. Ziegler, *J. Chem. Theory Comput.*, 2009, **5**, 962-975.
20.   A. Michalak, M. Mitoraj and T. Ziegler, *J. Phys. Chem. A*, 2008, **112**, 1933-1939.
21.   J.-X. Zhang, F. K. Sheong and Z. Lin, *Chem. Eur. J.*, 2018, **24**, 9639-9650.
22.   *M. J. Frisch, et al., Gaussian Inc., Wallingford CT, 2009.*
23.   D. Y. Zubarev and A. I. Boldyrev, *Phys. Chem. Chem. Phys.*, 2008, **10**, 5207-5217.
24.   P. v. R. Schleyer, C. Maerker, A. Dransfeld, H. Jiao and N. J. R. van Eikema Hommes, *J. Am. Chem. Soc.*, 1996, **118**, 6317-6318.

Table S1. Fully optimized structures of AnB$_8^-$ (An = Ac, Pa, Bk, Md, No) at PBE0/TZP level. Two types of isomers with pseudo-C_{7v} and C_s symmetries were tested.

AcB$_8^-$:

C_{7v}:

1.B	-0.396970	1.739241	1.762143
2.B	1.112287	1.394763	1.762143
3.B	1.783969	0.000000	1.762143
4.B	0.000000	0.000000	2.052902
5.B	1.112287	-1.394763	1.762143
6.B	-0.396970	-1.739241	1.762143
7.B	-1.607301	-0.774035	1.762143
8.B	-1.607301	0.774035	1.762143
9.Ac	0.000000	0.000000	-0.821402

C_s:

1.B	1.517408	1.691716	-0.801224
2.B	1.692653	0.367626	-1.637180
3.B	1.617565	-1.099883	-0.995673
4.B	2.138835	0.353116	0.000000
5.B	0.771496	-2.058595	0.000000
6.B	1.617565	-1.099883	0.995673
7.B	1.692653	0.367626	1.637180
8.B	1.517408	1.691716	0.801224
9.Ac	-0.685742	-0.006998	0.000000

PaB$_8^-$:

pseudo-C_{7v}:

1.B	1.556053	-0.396179	-1.719487
2.B	1.358409	-1.617108	-0.781228
3.B	1.358409	-1.617108	0.781228
4.B	1.923721	-0.001767	0.000000
5.B	1.556053	-0.396179	1.719487
6.B	1.475340	1.115520	1.384923
7.B	1.312703	1.810371	0.000000
8.B	1.475340	1.115520	-1.384923
9.Pa	-0.663786	-0.000631	0.000000

C_s:

1.B	1.386176	1.680257	-0.795607
2.B	1.546469	0.362160	-1.627389
3.B	1.529131	-1.088204	-0.955225
4.B	2.075723	0.361909	0.000000
5.B	0.560599	-1.967047	0.000000
6.B	1.529131	-1.088204	0.955225
7.B	1.546469	0.362160	1.627389

8.B	1.386176	1.680257	0.795607
9.Pa	-0.636608	-0.011234	0.000000

BkB$_8^-$:
pseudo-C_{7v}:

1.B	1.678401	-1.610967	-0.775258
2.B	1.678401	-1.610967	0.775258
3.B	1.670734	-0.397316	1.743286
4.B	1.930545	0.000009	0.000000
5.B	1.679962	1.114499	1.398832
6.B	1.667617	1.785984	0.000000
7.B	1.679962	1.114499	-1.398832
8.B	1.670734	-0.397316	-1.743286
9.Bk	-0.701362	-0.000037	0.000000

C_s:

1.B	1.329968	1.682028	-0.797744
2.B	1.535546	0.365358	-1.626662
3.B	1.456997	-1.094836	-0.979452
4.B	2.020881	0.365893	0.000000
5.B	0.540712	-1.999899	0.000000
6.B	1.456997	-1.094836	0.979452
7.B	1.535546	0.365358	1.626662
8.B	1.329968	1.682028	0.797744
9.Bk	-0.619564	-0.009360	0.000000

MdB$_8^-$:
pseudo-C_{7v}:

1.B	1.734964	1.583460	-0.775857
2.B	1.704207	0.369393	-1.742238
3.B	1.677811	-1.144113	-1.397312
4.B	1.943643	-0.033297	0.000000
5.B	1.673142	-1.818789	0.000000
6.B	1.677811	-1.144113	1.397312
7.B	1.704207	0.369393	1.742238
8.B	1.734964	1.583460	0.775857
9.Md	-0.732265	0.012428	0.000000

C_s:

1.B	1.639508	1.651446	-0.787871
2.B	1.630726	0.300382	-1.624246
3.B	1.688214	-1.182406	-0.942847
4.B	2.142410	0.255847	0.000000
5.B	1.618706	-2.473576	0.000000
6.B	1.688214	-1.182406	0.942847

7.B	1.630726	0.300382	1.624246
8.B	1.639508	1.651446	0.787871
9.Md	-0.724893	0.031387	0.000000

NoB$_8^-$:

C_{7v}:

1.B	-0.398106	1.744215	-1.561657
2.B	-1.611897	0.776249	-1.561657
3.B	-1.611897	-0.776249	-1.561657
4.B	0.000000	0.000000	-1.799432
5.B	-0.398106	-1.744215	-1.561657
6.B	1.115467	-1.398752	-1.561657
7.B	1.789070	0.000000	-1.561657
8.B	1.115467	1.398752	-1.561657
9.No	0.000000	0.000000	0.880527

C_s:

1.B	1.651306	1.661301	-0.788052
2.B	1.636646	0.309283	-1.624381
3.B	1.693222	-1.175176	-0.942857
4.B	2.144358	0.263743	0.000000
5.B	1.629202	-2.466445	0.000000
6.B	1.693222	-1.175176	0.942857
7.B	1.636646	0.309283	1.624381
8.B	1.651306	1.661301	0.788052
9.No	-0.726935	0.028401	0.000000

Table S2. Relative energies of different electronic structures of AnB_8^- (An = Ac, Pa, Bk, Md, No) at PBE/TZP and PBE0/TZP levels.

Species	An atomic electronic configuration	2S+1	PBE	PBE0
AcB_8^-	s^2	1	0.00	0.00
	d^1s^1	3	5.15	6.98
	d^2	3	27.70	-
PaB_8^-	$f^1d^2s^1$	5	0.00	0.00
	$f^2d^1s^1$	5	3.32	2.20 (4.11)[a]
	f^2s^2	3	7.64	4.73
BkB_8^-	f^9s^1	7	0.00	0.00
	f^8s^2	7	2.53	4.19 (2.99)[a]
	$f^7d^1s^1$	9	26.46	24.13
MdB_8^-	$f^{13}s^1$	3	0.00	0.00
	$f^{12}s^2$	3	40.41	46.78
	$f^{12}d^1s^1$	5	59.33	62.79
NoB_8^-	$f^{14}s^1$	2	0.00	0.00
	$f^{14}d^1$	2	42.84	43.38
	$f^{13}d^1s^1$	4	119.57	133.13

[a] The energies are obtained from CASSCF/NEVPT2/SO calculations.
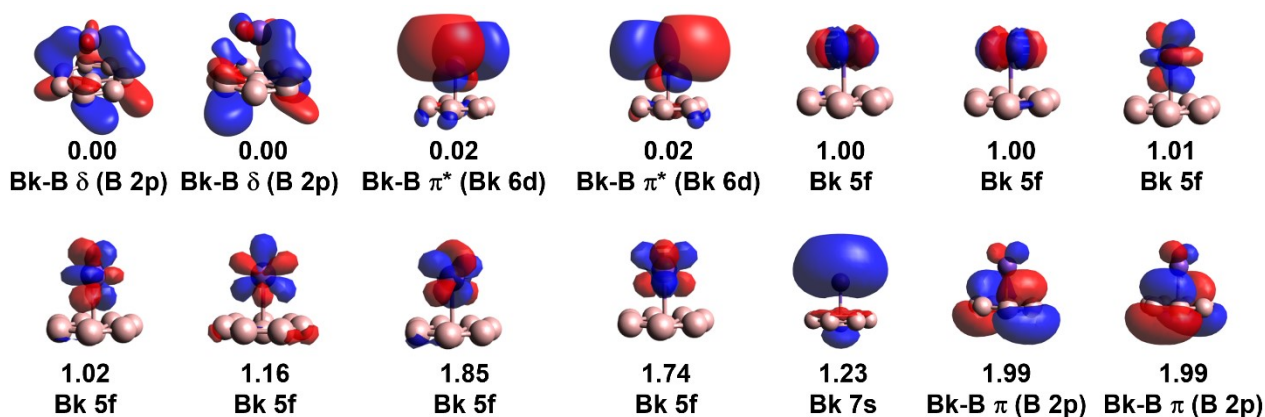
Fig. S1. Natural orbital occupations of BkB_8^- obtained from a CASSCF (14e, 14o) calculation at the PBE0/TZP optimized geometry, with the consideration of SOC effect. The dominant contributions are indicated for each orbital. The CI coefficient for Bk (+I) ($5f^97s^1$) is 76%, with a 22% mixture of Bk (+I) ($5f^87s^2$).
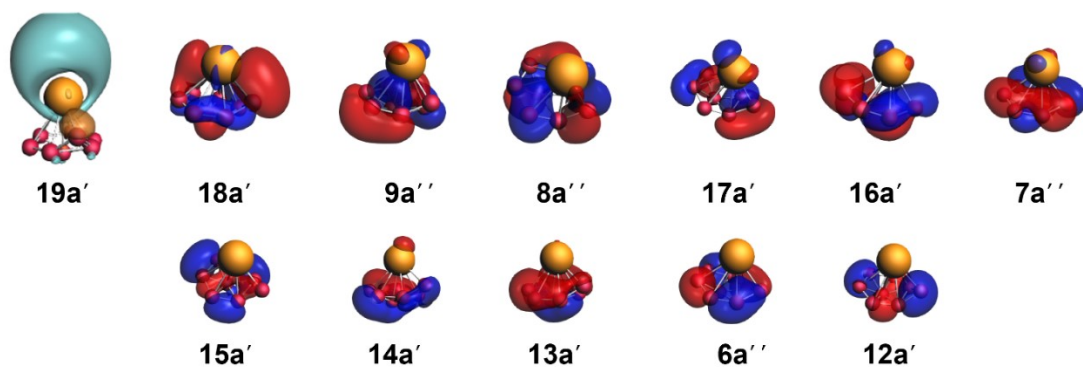
Fig. S2. Frontier orbital contours (isovalue = 0.03 a.u.) of AcB_8^- with trivalent Ac (+III) OS at PBE0/TZVP level.
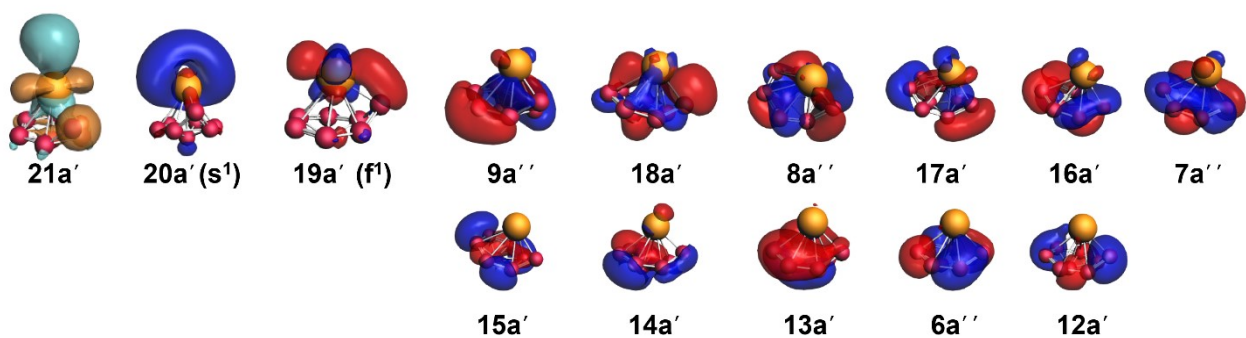
Fig. S3. Frontier orbital contours (isovalue = 0.03 a.u.) of PaB_8^- with trivalent Pa (+III, f^1s^1) OS at PBE0/TZVP level.

	1st PIO	2nd PIO	3rd PIO	4th PIO	
(a) Frag A (Ac⁻)					
Frag B (B_8^{2-})					
PIO (contrib%)	32.96%	24.88%	24.88%	7.67%	
cum%	32.96%	57.84%	82.72%	90.39%	

	1st PIO	2nd PIO	3rd PIO	4th PIO	5th PIO
(b) Frag A (Pa⁺)					
Frag B (B_8^{2-})					
PIO (contrib%)	25.11%	22.71%	16.15%	14.40%	7.04%
cum%	25.11%	47.81%	63.96%	78.36%	85.41%

	1st PIO	2nd PIO	3rd PIO	4th PIO	5th PIO
(c) Frag A (Bk⁺)					
Frag B (B_8^{2-})					
PIO (contrib%)	25.63%	25.63%	17.54%	16.45%	4.39%
cum%	25.63%	51.26%	68.80%	85.25%	89.64%

	1st PIO	2nd PIO	3rd PIO	4th PIO	5th PIO
(d) Frag A (Md⁺)					
Frag B (B_8^{2-})					
PIO (contrib%)	30.45%	26.62%	18.68%	11.26%	2.38%
cum%	30.45%	57.07%	75.75%	87.01%	89.39%

Fig. S4. The results of PIO analysis on the AnB_8^-(An = Ac, Pa, Bk, Md and No) at the PBE0/ECP60MWB/6-311G* level with An^+ and B_8^{2-}as two fragments. The contribution of first six dominant PIO (contrib%) and cumulative contribution (cum%) to the total interactions between two fragments are shown. The isovalue for each orbital is 0.02 a.u.
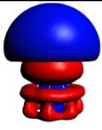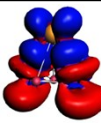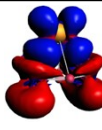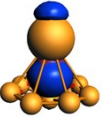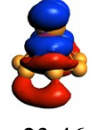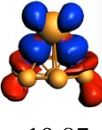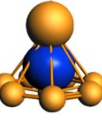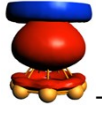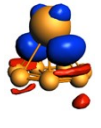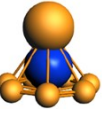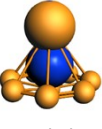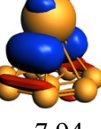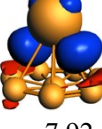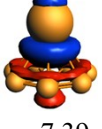
Table S3. The EDA-NOCV results for the AnB_8^- (An = Ac, Pa, Bk, Md and No) at the PBE0/TZP level. The scalar relativistic (SR) effects were taken into account according to the zero-order regular approximation (ZORA). (Energy values are given in kcal/mol, $\Delta E_{int} = \Delta E_{Pauli} + \Delta E_{elstat} + \Delta E_{orb}$).

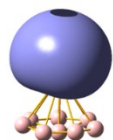| Fragments	Ac^+ $(7s^2)$ $+ B_8^{2-}$ $(^1A')$	Pa^+ $(5f^16d^27s^1)$ $+ B_8^{2-}$ $(^1A')$	Bk^+ $(5f^97s^1)$ $+ B_8^{2-}$ $(^1A')$	Md^+ $(5f^{13}7s^1)$ $+ B_8^{2-}$ $(^1A')$	No^+ $(5f^{14}7s^1)$ $+ B_8^{2-}$ $(^1A')$
ΔE_{int}	-275.51	-305.91	-245.72	-297.66	-239.10
ΔE_{pauli}	176.76	318.70	143.24	107.89	102.40
ΔE_{elstat}[a]	-309.79 (69.33%)	-395.86 (63.38%)	-288.79 (74.24%)	-266.24 (65.65%)	-262.44 (76.85%)
ΔE_{orb}[a]	-138.47 (30.67%)	-228.75 (36.62%)	-100.18 (25.76%)	-139.30 (34.35%)	-79.05 (23.15%)
$\Delta E_{orb(1)}$[b]	-44.11 (31.86%)	-46.66 (20.40%)	-23.90 (23.86%)	13.42 (-9.63%)	-26.39 (33.38%)
$\Delta E_{orb(2)}$[b]	-31.97 (23.09%)	-42.24 (18.47%)	-14.28 (14.25%)	-17.35 (12.46%)	-16.38 (20.72%)
$\Delta E_{orb(3)}$[b]	-31.93 (23.06%)	-30.12 (13.17%)	-21.84 (21.81%)	-28.95 (20.79%)	-15.83 (20.02%)
$\Delta E_{orb(4)}$[b]	-9.67 (6.98%)	-35.60 (15.56%)	-15.38 (15.35%)	-16.82 (12.07%)	-7.29 (9.22%)
$\Delta E_{orb(5)}$[b]	-4.09 (2.95%)	-29.13 (12.74%)	-8.70 (8.68%)	-14.11 (10.13%)	-2.49 (3.15%)
$\Delta E_{orb(6)}$[b]	-4.09 (2.95%)	-20.50 (8.96%)	-4.18 (4.17%)	-17.79 (12.77%)	-2.49 (3.15%)
$\Delta E_{orb(7)}$[b]	-2.96 (2.14%)	-8.70 (3.81%)	-2.21 (2.20%)	-17.51 (12.57%)	/
$\Delta E_{orb(8)}$[b]	-2.59 (1.87%)	-3.71 (1.62%)	-2.13 (2.13%)	-13.82 (9.92%)	/
$\Delta E_{orb(9)}$[b]	-2.59 (1.87%)	-2.84 (1.24%)	-2.36 (2.36%)	-13.64 (9.79%)	/
ΔE_{rest}[b]	-4.47 (3.23%)	-9.24 (4.04%)	-5.19 (5.18%)	-12.72 (9.13%)	-8.19 (10.36%)

[a] The values in parentheses provide the percentage contribution to the total attractive interactions $\Delta E_{elstat} + \Delta E_{orb}$.
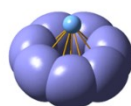[b] The values within the parentheses show the contribution to the total orbital interaction.

Table S4. The deformation densities (Δρ, isosurface=0.0005) of the dominant pairwise orbital interactions of EDA-NOCV analysis (charge density flow from red to blue) of AnB_8^- at the PBE0/TZP level. The energies in kcal/mol.

		s	d/d-p δ		d-p π		d-p σ
AcB_8^-		-44.11			-31.97	-31.93	-9.67
PaB_8^-	α	-30.46	-28.33	-35.55	-24.84	-16.04	-11.17
	β				-23.46	-19.87	-10.83
BkB_8^-	α	-22.07			-12.00	-11.84	-6.06
	β				-4.17	-7.47	-5.99
MdB_8^-	α	19.13			-8.97	-8.80	-4.68
	β				32.55	-8.38	-20.15
NoB_8^-	α	-18.44			-8.46	-8.44	-4.45
	β				-7.94	-7.92	-7.39

(a) AcB$_8^-$

1c-1e Ac 7s
ON = 2.00

7 × 2c-2e B–B bonds
ON = 1.94

3 × 9c-2e σ bonds
ON = 2.00
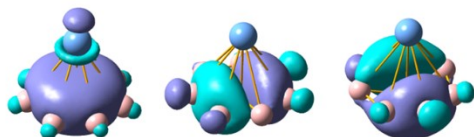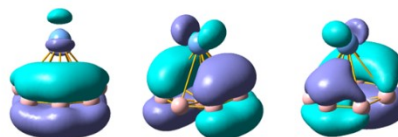
3 × 9c-2e π bonds
ON = 2.00

(b) PaB$_8^-$
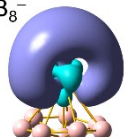
1c-1e Pa 7s
ON = 0.92
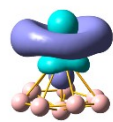
1c-1e Pa 5f
ON = 1.00
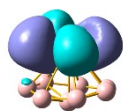
2 × 1c-1e Pa 6d
ON = 0.62~0.68
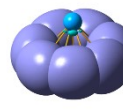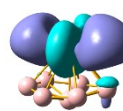
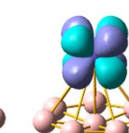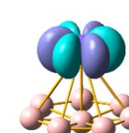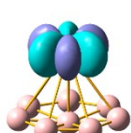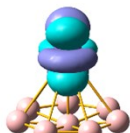7 × 2c-2e B–B bonds
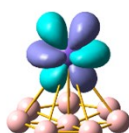ON = 1.92

3 × 9c-2e σ bonds
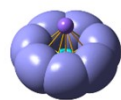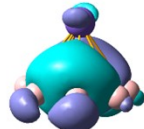ON = 2.00
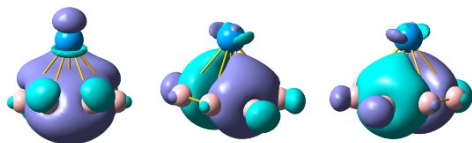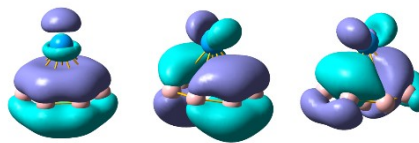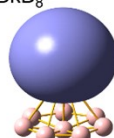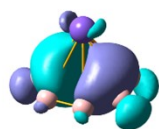
3 × 9c-2e π bonds
ON = 2.00
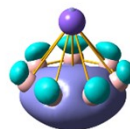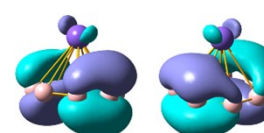
(c) BkB$_8^-$

1c-1e Bk 7s
ON = 1.00
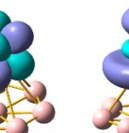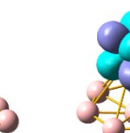
5 × 1c-1e Bk 5f
ON = 1.00

2 × 1c-2e Bk 5f
ON = 1.94~1.98

7 × 2c-2e B–B bonds
ON = 1.94

3 × 9c-2e σ bonds
ON = 2.00

3 × 9c-2e π bonds
ON = 2.00

(d) MdB$_8^-$

1c-1e Md 7s
ON = 1.03

6 × 1c-2e Md 5f
ON = 1.99~2.00

1c-1e Md 5f
ON = 1.01

7 × 2c-2e B–B bonds
ON = 1.94

3 × 9c-2e σ bonds
ON = 2.00

3 × 9c-2e π bonds
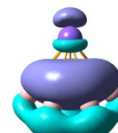ON = 2.00

(e) NoB$_8^-$

1c-1e No 7s
ON = 1.04

7 × 1c-2e No 5f
ON = 2.00

7 × 2c-2e B–B bonds
ON = 1.94

3 × 9c-2e σ bonds
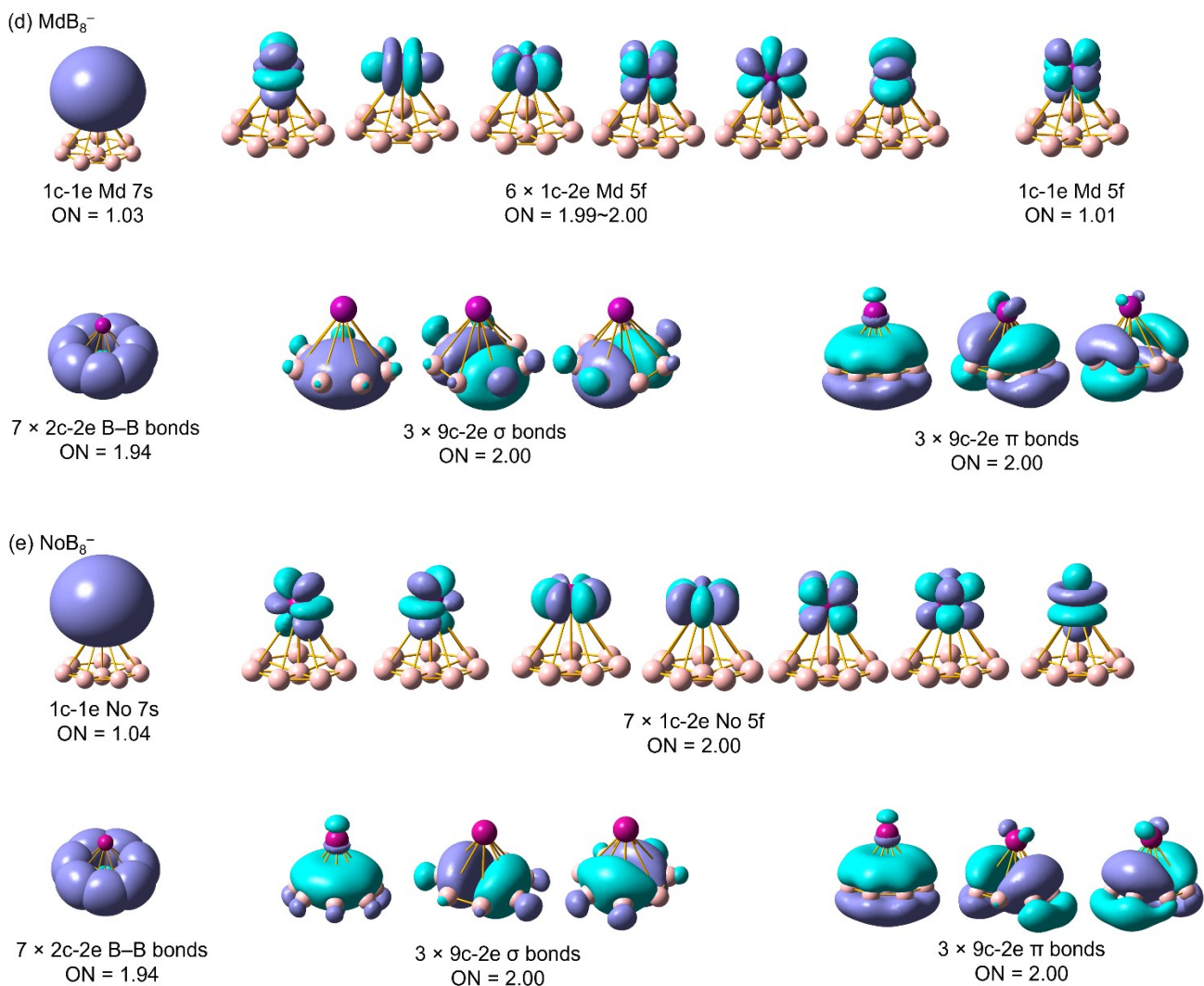ON = 2.00

3 × 9c-2e π bonds
ON = 2.00

Fig. S5. AdNDP delocalized bonding analyses of AnB$_8^-$ (An = Ac, Pa, Bk, Md, No) at PBE0/VTZ level.

Table S5. The NICS indices of AnB$_8^-$(An=Ac, Pa, Bk, Md and No) calculated at the PBE0/ECP60MWB/6-311G* level, at the center B of B$_8$ ring.

	NICS (0)	NICS (1)
AcB$_8^-$	-57.24	-0.56
PaB$_8^-$	-54.75	-14.23
BkB$_8^-$	-102.44	-33.41
MdB$_8^-$	-82.38	-23.10
NoB$_8^-$	-83.89	-22.97

Table S6. Different B-B distances in AnB_8^-(An=Ac, Pa, Bk, Md and No) at PBE0/TZP level.

	Peripheral B-B	Radial B-B
AcB_8^-	1.553 ± 0.009	1.820 ± 0.014
PaB_8^-	1.555 ± 0.004	1.850 ± 0.039
BkB_8^-	1.551 ± 0.001	1.806 ± 0.001
MdB_8^-	1.552 ± 0.003	1.805 ± 0.001
NoB_8^-	1.552 ± 0.000	1.805 ± 0.000